

Large-Area Ohmic Top Contact to Vertically Grown Nanowires Using a Free-Standing Au Microplate Electrode

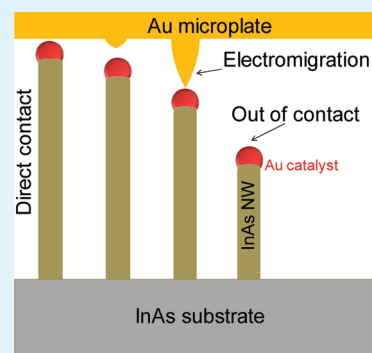
B. Radha,[†] Deepak Jayaraj,[†] G. U. Kulkarni,^{*,†} Stefan Heun,[‡] Daniele Ercolani,[‡] and Lucia Sorba[‡]

[†]Chemistry and Physics of Materials Unit and DST Unit on Nanoscience, Jawaharlal Nehru Centre for Advanced Scientific Research, Jakkur P. O., Bangalore 560 064, India

[‡]NEST, Istituto Nanoscienze-CNR and Scuola Normale Superiore, Piazza San Silvestro 12, 56127 Pisa, Italy

S Supporting Information

ABSTRACT: A method of electrically contacting vertically grown nanowires of uneven heights, a common scenario among as-grown nanowires, is reported here using a chemically synthesized single-crystalline Au microplate as top electrode. The contact is electrically activated and the contact formation is predominantly due to electromigration. With this approach, the electrode could ohmically contact several thousand nanowires at once.



KEYWORDS: top contacts, vertical nanowires, Au microplate, ohmic contact, single-crystalline electrode

INTRODUCTION

One-dimensional structures such as carbon nanotubes and semiconductor nanowires (NWs) are explicitly foreseen as realistic candidates for modern electronic applications.¹ Vertically grown nanotubes and NWs especially are of paramount importance in applications such as energy storage,² sensing,³ power generation,⁴ light-emitting diodes,⁵ and solid state lighting.⁶ Voltage generation using piezoresponsive materials has also been shown to be most effective in vertical geometry.⁷ Although contacting every individual NW and sourcing the tiny charge or signal from it are important for effective usage in technological applications,⁸ it is extremely challenging to employ the pick-and-place method in routine device fabrication. Thus, top-contacting vertically grown NWs is still a pertinent issue in the literature.¹ Although drawing individual contacts out is desirable, it is not usually required; a canopy of networked contacts serves most applications. An additional complication is often posed by the typically large variation in the heights of the vertical NWs.^{9,10} In this work, the top contacting of an array of vertically grown NWs of varying heights is demonstrated while overcoming the fabrication drawbacks.

Top-contacting individual NWs has been achieved in the past using scanning probe techniques - conducting atomic force microscope^{11,12} and scanning tunneling microscope,¹³ and of late, nanoprobe¹⁴ and air-bridge connection.¹⁵ Although these techniques have been largely successful, they are time-consuming and, importantly, may not give rise to stand-alone devices. An alternate but somewhat compromising method is to top-contact a number of vertical NWs using large area

electrodes. Deposition of a metal film, say by physical vapor deposition, would not work as the metal seeps through the voids in between the NWs and shorts with the bottom electrode. In order to avoid this, the NWs are typically first embedded in a dielectric layer such as a polymer. Planarization is then performed to get NWs of the desired length.¹⁶ Following etching of the polymer to expose the tips of the NWs, a metal film is deposited on top as the contact pad.¹⁷ ZnO NW-based power generators have been realized by the above method. Recently, a flexible CNT film was used as a top electrode for pillared CuI structures in a solar cell.¹⁸ Here we report a simple, lithography free method that makes use of large, flat, single-crystalline Au hexagonal microplates to contact vertical NWs via electrical activation. As a case study, InAs NWs are used, which were grown by chemical beam epitaxy employing Au catalyst particles on an InAs(111)A substrate with trimethylindium and tert-butylarsine as metal-organic precursors.¹⁹ The Au catalyst particles have been realized by thermal dewetting of nominally 0.5 nm thick gold films. The resulting nanoparticles have a wide diameter range, which implies that the diameter of the NWs is varied, the mean value being 75 ± 14 nm. The NW growth is Au-assisted, with a Au catalyst particle at the top of each NW.¹⁹ The as-grown NWs are not of the same height, the mean height being $0.600 \mu\text{m}$ with a relatively large variation of $\pm 0.250 \mu\text{m}$. Although setting top contact with the tallest NWs could be achieved by just

Received: January 12, 2012

Accepted: March 16, 2012

Published: March 16, 2012

placing a flat electrode, the NWs of smaller heights pose a challenge. This article describes a method of bringing even shorter NWs into ohmic contact. The nanowire sample in this study was chosen to have a broad distribution in the height of the nanowires and the effort was to bring maximum number of nanowires into contact.

RESULTS AND DISCUSSION

The Au microplates that serve as top electrodes in this study were synthesized by a process developed by the authors,²⁰ which involves drop coating a Au-organic complex, i.e., $(\text{AuCl}_4)^-$ anions stabilized by tetraoctylammonium bromide in toluene (25 mM, 100 μL), on a glass substrate and thermolyzing at 130 $^\circ\text{C}$ for 24 h in air. The microplates were large, extending to several thousand square micrometers and atomically flat with surface roughness <1 nm.²¹ The microplates (area up to $\sim 12\,000$ μm^2) were freed from the substrate by sonicating in toluene. In order to make the electrical connection to the Au microplate, a conducting carbon fiber (diameter 6 μm and length 2 mm) coated with Pd hexadecylthiolate as a soldering precursor was placed with its one end spanning across a large hexagonal microplate, and the setup was heated to 250 $^\circ\text{C}$ for 60 min to cause metallization of the precursor and hence soldering²² (see Figure 1b). The device consists of a clean glass slide as the base for the InAs substrate carrying InAs NWs and a Au (~ 40 nm thick) coated glass slide (of similar thickness as the InAs substrate, ~ 300 μm) juxtaposed with a separation of several tens of μm s for electrical isolation (see Figure 1a). Both the height of NWs and the thickness of Au coating are insignificant compared to the thickness of substrates and therefore are not critical process parameters. Such small differences were taken care by the bending of the long C-fiber. The arrangement was such that the C-fiber contacted the Au microplate electrode only from the top and no NWs directly. The soldered Au microplate was lifted by holding the fiber from the free end, manually using a 3-axis micromanipulating tool (Nanomax TS) and placed gently onto the InAs substrate such that the microplate rested on the NWs (Figure 1c), and the free end of the fiber on the Au coated glass slide. Subsequently, the latter was also soldered using a drop of the Pd precursor. Thus a sandwich device comprising Au microplate/InAs NWs/InAs substrate was made. The density of the NWs was measured to be ~ 12 μm^{-2} , and given that the area of the microplate used for the experiment was ~ 1000 μm^2 , the total number of NWs under the microplate comes out to be $\sim 12\,000$. From the SEM image in Figure 1c, one may visualize the NWs underneath the microplate edges indicating that they preserve the contact without being mechanically crushed. This can be rationalized by considering that the critical load for an ideal elastic column, often called the Euler load for failure²³ due to buckling, is given by $P = \pi^2 EI/L_e^2$ where E is Young's modulus and the moment of inertia, $I = \pi R^4/4$, R is diameter of the NW. The effective length L_e is $L_e = KL$, where L is the actual length of the column or the nanowire, and K is column effective length factor (for one end fixed and the other end pinned, $K \approx 0.7$). The buckling behavior of NWs in this work can be approached by considering the NW to be a nanocolumn fixed at the base and pinned at the top (usually called a fixed pinned column), where $P = 2.04\pi^2 EI/L^2$. The critical load for a single InAs NW (dia, ~ 75 nm; height, 1 μm), calculated according to the Euler load for failure turns out to be 2×10^{-4} N. The top Au plate

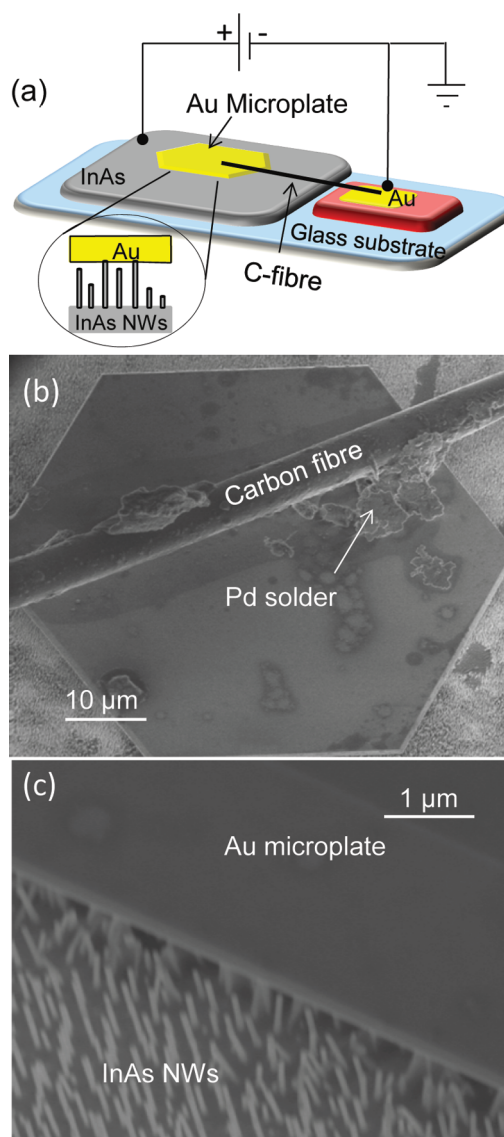


Figure 1. (a) Schematic showing the device configuration of Au microplate/InAs NW sandwich. (b) SEM image of the actual sandwich device, with the clear image of the soldered point between Au microplate and C-fiber with the Pd solder trace. The Pd metal in between the carbon fiber and the microplate is also clearly evident. (c) InAs NWs beneath the Au microplate captured along the edges (imaging done at tilt angle of 60°).

corresponds to a load of 3×10^{-27} N per NW, safely below the critical value.

The prevalent contact by the tallest NWs produced a tiny current of ~ 37 nA, when 0.5 mV bias was applied to the InAs substrate carrying the NWs (the Au microplate was held at ground potential, see Figure 1a). The current got stabilized at ~ 84 nA after 45 s. The total resistance of the NWs in contact works out to be 5.9 k Ω , and considering the known approximate resistance of the individual NW (~ 25 k Ω),²⁴ the fraction of NW in contact is only $\sim 0.04\%$ of the total number of NWs under the microplate electrode. According to the height distribution histogram of the NWs (see the Supporting Information, Figure S1), this corresponds to the tallest NWs and those which fall short of that height by a few nm. Little distortions may be caused by the microplate in contact, which evens out the small differences in heights of NWs. With the

voltage on (0.5 mV), the current through the sandwich device began to increase with time which implies either opening up of more conducting channels or annealing of the set contacts, or both. This aspect was studied in detail (Figure 2). In the initial

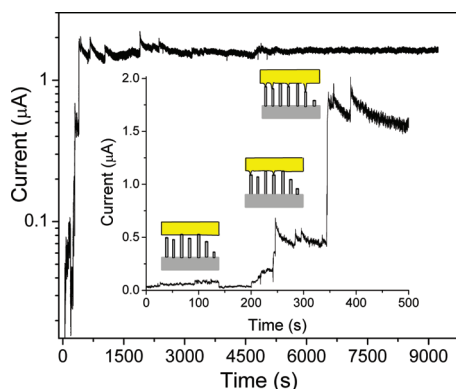


Figure 2. Current of the sandwich device recorded as a function of time, applying 0.5 mV for current induced electrical activation at a data collection rate of 1000 points per second for more than 9000 s. Note the logarithmic current scale. Inset shows zoom-in for the first 500 s (linear current scale) and schematic illustrations at various stages of NWs establishing contact with the top microplate electrode.

240 s, the current increased gradually to 179 nA and jumped to 672 nA at around 246 s. Although a gradual increase may be taken to represent annealing of set contacts, a jump in current may correspond to more NWs coming in contact with the top electrode. The NWs, which are within a short distance from the top electrode, could be electrically contacted, and going by a similar estimate as before, this fraction comes out to be $\sim 0.3\%$ of the total. This type of contact can be visualized as analogous to atomic wire formation observed in STM studies,²⁵ under an applied bias between a sharp tip and a flat substrate (Au nanoparticle terminated InAs NW as “tip” and the Au microplate as the ‘substrate’ respectively, in the present case). Further continued application of the bias led to a sudden rise in the current from 0.82 to 1.87 μA at about ~ 344 s. Such

noticeable rise in current indicates that a large number of NWs came into contact. It was estimated that $\sim 1\%$ of all NWs are in contact at this point (see the schematic illustration in the inset of Figure 2). In terms of distance from the microplate, this fraction covers a range of few tens of nm, from the Au nanoparticle tip (see Figure S1 in the Supporting Information). Given such large distances, it is reasonable to think that an electromigration process may be responsible—from microplate electrode to the Au nanoparticle tip. Such stalactite formation from the electrodes has been discussed in the context of molecular systems,²⁶ although the distances involved in those cases are much smaller. Indeed, electromigration, i.e., migration of metal under applied field is considered as a serious mode of failure in printed circuit boards as it forms shorts.²⁷ Usually in electromigration, dendritic or stalactite filaments grow towards the positive electrode in an applied DC field.²⁸ From Figure 2, it may be seen that the current eventually settles around $\sim 1.8 \mu\text{A}$ but for small sudden variations. This marks the stabilization of the contact between the microplate electrode and the NWs. There may be instances of incomplete electromigration with the Au stalactites being very close but not yet contacting the InAs NWs, and in such cases tunneling may also be a contributing factor for overall conduction. As the measurements of nanowire height are based on SEM, nanometric accuracy was not possible. Tunneling, if exists, is relevant within 1 nm, and given the accuracy of heights measured, no concrete conclusions can be drawn with regard to the role of tunneling in transport. Further, tunneling will contribute in the range of few nanoamps while jumps in current observed are tens to hundreds of nanoamps. However, much shorter NWs could not make it owing to large gaps from the electrode. The latter fraction is astonishingly high, $\sim 99\%$!

The device was dismantled and the microplate surface which was in contact with the NWs, was examined (Figure 3). In contrast to the smooth pristine surface (Figure 3a), the surface after contacting, is filled with bright features in the AFM topography image (see Figure 3b). These features represent local topographical deviations from the atomically flat surface. The AFM image (shown upside down) in Figure 3c clearly

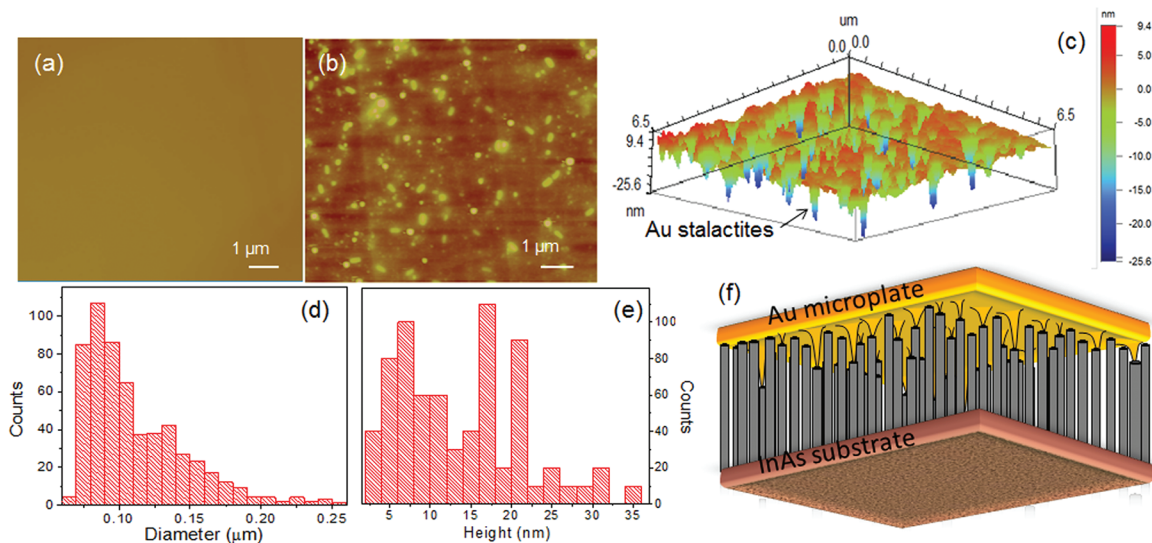


Figure 3. AFM images of the Au microplate top electrode surface, (a) before and (b) after electrical activation. (c) Planar view of stalactites on Au microplate surface (Image is turned upside down for better understanding). (d, e) Histograms of the stalactites tip diameter and height. (f) Schematic of the sandwich device with the microplate/InAs NWs and the developed stalactites.

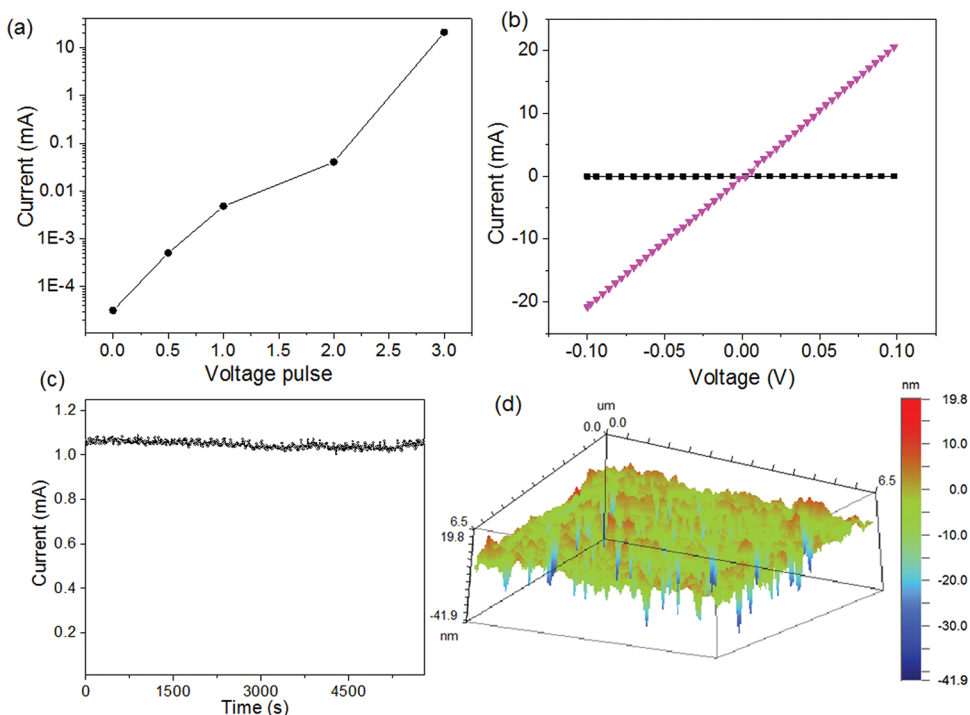


Figure 4. Voltage-induced electrical activation: (a) Current at 0.1 V plotted versus the voltage pulse used for contact initiation. All pulses were of duration ~ 10 s. (b) I - V characteristics of the sandwich device, before (squares) and after applying a voltage pulse of 3 V (triangles). When 3 V was pulsed for 10 s, the current improved significantly. (c) Current-time plot showing the retention of the contact of the NWs (read voltage, 5 mV). (d) AFM planar image of stalactites on Au microplate surface (image is shown upside down).

shows the stalactites pointing down with lengths up to ~ 25 nm. From the histogram in Figure 3d, the mean tip diameter of the stalactite filament is ~ 70 nm, which corresponds roughly to the average diameter of the individual InAs NWs (~ 75 nm). The height histogram of the stalactites which could be responsible for the contact with NWs is shown in Figure 3e. The stalactite induced contact is illustrated more vividly in Figure 3f. Good agreement between the results of Figures 2 and 3 is observed: stalactites with a length of up to 25 nm were found, and NWs with a maximum distance from the microplate of a few tens of nanometers are contacted. Also, the NW tips were examined for evidence of any sharp dendritic or stalactite features originating from the catalyst particles on the heads of InAs NWs (see Figure S2 in the Supporting Information); microscopy indicates that the NWs and the catalyst particles at the tips of NWs are intact without any deformation. Also, the stalactites' magnitude is too large to originate from the catalyst particle. Thus, the stalactite contacts predominantly originate from the Au microplate electrode only. This corroborates our interpretation.

The above method of applying a tiny bias (0.5 mV) and observing the current through the device with time was carried out essentially to understand the contacting process. While the above results gave an insight into the process, finally, only 1% of NWs could be brought into electrical contact, and this over a period of ~ 50 min! To increase the yield of contacted NWs, increasing the bias and applying it continuously (see Figure S3 in the Supporting Information) would not do as the current carrying capacity of NWs is limited. It is reported that NWs start melting when the joule heat generated locally exceeds typically a few tens to hundreds of μW .²⁹ In order to avoid such a situation, we switched from a continuous application of voltage to short bias pulses. For a given sample to reach its

steady state condition, the required voltage was determined empirically by applying short (10 s) voltage pulses starting from 0.5 up to 3 V. The state of the device after pulsing was examined using a reading voltage of 0.1 V (Figure 4a). Initially after pulsing with 0.5 V, the current was low (~ 510 nA) and nonlinear. By increasing the pulsing voltage, not only there was an increase in the current (see Figure 4a) but also nearly linear I - V behavior was achieved as shown in Figure 4b. Thus a higher voltage (3 V) in short pulses (10 s) was applied leading to success in bringing $\sim 50\%$ of the NWs into ohmic contact (see linear behavior in Figure 4b). These contacts were robust, because the current remained steady (1.08 ± 0.02 mA at 5 mV) even after 100 min (see Figure 4c). A further increase in voltage (4 V) did not improve the number of NWs coming into contact significantly. This is an empirical observation and the conditions of pulsing voltage may vary depending on the density of the NWs, area of the microplate, height distribution of the NWs etc. The swiftness of the contact development in this case indicates that the above-discussed processes — direct contact and electromigration — take place simultaneously. The microplate electrode surface from this device indeed showed stalactites which are more longer (up to ~ 62 nm) with a higher density (Figure 4d). The fraction of NW in contact achieved by this process can be compared with that obtained with the airbridge¹⁵ or the planarization method.¹⁶

CONCLUSIONS

In conclusion, a simple method for top contacting a large number of NWs in vertical geometry has been devised using a mesoscopic Au electrode. In spite of widely distributed heights of the NWs, almost 50% of the NWs were brought into contact without damage. The surface of NWs is free and can be exposed to gases for specific applications in contrast to

conventional top-contact methods where NWs are constrained in a dielectric polymer environment. This method is distinctly different in that it is lithography-free and does not require sophisticated nanomanipulation techniques. The device is essentially self-standing, which paves the way to up-scale circumventing the stumbling block for the development of NWs/nanotubes from growth to applications.

■ ASSOCIATED CONTENT

● Supporting Information

SEM image of the InAs NWs with height histogram; SEM images of the NWs after electrical analysis; current–time characteristics of the NW sandwich device at various applied constant bias (PDF). This material is available free of charge via the Internet at <http://pubs.acs.org/>.

■ AUTHOR INFORMATION

Corresponding Author

*Telephone: +91-80-2208 2814. Fax: +91-80-2208 2766. E-mail: kulkarni@jncasr.ac.in.

Notes

The authors declare no competing financial interest.

■ ACKNOWLEDGMENTS

We acknowledge financial support from Monte dei Paschi di Siena with the project “Implementazione del laboratorio di crescita dedicato alla sintesi di nanofili a semiconduttore”, FIRB project prot. RBIN067A39_002, and the Indo-Italian POC in S&T 2008–2010. B.R. thanks CSIR (India) for her fellowship. G.U.K. thanks DST, India, for project support. Discussions with S. Roddaro and A. Pitanti are gratefully acknowledged.

■ REFERENCES

- (1) Thelander, C.; Agarwal, P.; Brongersma, S.; Eymery, J.; Feiner, L. F.; Forchel, A.; Scheffler, M.; Riess, W.; Ohlsson, B. J.; Goesele, U.; Samuelson, L. *Mater. Today* **2006**, *9*, 28.
- (2) Gowda, S. R.; Leela Mohana Reddy, A.; Zhan, X.; Ajayan, P. M. *Nano Lett.* **2011**, *11*, 3329.
- (3) Field, C. R.; In, H. J.; Begue, N. J.; Pehrsson, P. E. *Anal. Chem.* **2011**, *83*, 4724.
- (4) Choi, D.; Choi, M.-Y.; Shin, H.-J.; Yoon, S.-M.; Seo, J.-S.; Choi, J.-Y.; Lee, S. Y.; Kim, J. M.; Kim, S.-W. *J. Phys. Chem. C* **2010**, *114*, 1379.
- (5) Lai, E.; Kim, W.; Yang, P. *Nano Res.* **2008**, *1*, 123.
- (6) Li, Q.; Wang, G. T. *Nano Lett.* **2010**, *10*, 1554.
- (7) Xu, S.; Qin, Y.; Xu, C.; Wei, Y.; Yang, R.; Wang, Z. L. *Nanotechnol.* **2010**, *5*, 366.
- (8) Freer, E. M.; Grachev, O.; Duan, X.; Martin, S.; Stumbo, D. P. *Nat. Nanotechnol.* **2010**, *5*, 525.
- (9) Jensen, L. E.; Björk, M. T.; Jeppesen, S.; Persson, A. I.; Ohlsson, B. J.; Samuelson, L. *Nano Lett.* **2004**, *4*, 1961.
- (10) Roddaro, S.; Caroff, P.; Biasiol, G.; Rossi, F.; Bocchi, C.; Nilsson, K.; Fröberg, L.; Wagner, J. B.; Samuelson, L.; Wernersson, L.-E.; Sorba, L. *Nanotechnol.* **2009**, *20*, 285303.
- (11) Erts, D.; Polyakov, B.; Daly, B.; Morris, M. A.; Ellingboe, S.; Boland, J.; Holmes, J. D. *J. Phys. Chem. B* **2005**, *110*, 820.
- (12) Moutanabbir, O.; Senz, S.; Scholz, R.; Alexe, M.; Kim, Y.; Pippel, E.; Wang, Y.; Wiethoff, C.; Nabbefeld, T.; Meyer zu Heringdorf, F.; Horn-von Hoegen, M. *ACS Nano* **2011**, *5*, 1313.
- (13) Talin, A. A.; Swartzentruber, B. S.; Leonard, F.; Wang, X.; Hersee, S. D. *J. Vac. Sci. Technol. B* **2009**, *27*, 2040.
- (14) Talin, A. A.; Léonard, F.; Katzenmeyer, A. M.; Swartzentruber, B. S.; Picraux, S. T.; Toimil-Molares, M. E.; Cederberg, J. G.; Wang, X.; Hersee, S. D.; Rishinaramangalum, A. *Semicond. Sci. Technol.* **2010**, *25*, 024015.
- (15) Offermans, P.; Crego-Calama, M.; Brongersma, S. H. *Nano Lett.* **2010**, *10*, 2412.
- (16) Chia, A. C. E.; LaPierre, R. R. *Nanotechnol.* **2011**, *22*, 245304.
- (17) Wang, X.; Kim, K.; Wang, Y.; Stadermann, M.; Noy, A.; Hamza, A. V.; Yang, J.; Sirbuly, D. J. *Nano Lett.* **2010**, *10*, 4901.
- (18) Li, P.; Wang, S.; Jia, Y.; Li, Z.; Ji, C.; Zhang, L.; Li, H.; Shi, E.; Bian, Z.; Huang, C.; Wei, J.; Wang, K.; Zhu, H.; Wu, D.; Cao, A. *Nano Res.* **2011**, *4*, 979.
- (19) Ercolani, D.; Rossi, F.; Li, A.; Roddaro, S.; Grillo, V.; Salviati, G.; Beltram, F.; Sorba, L. *Nanotechnol.* **2009**, *20*, 505605.
- (20) Radha, B.; Arif, M.; Datta, R.; Kundu, T.; Kulkarni, G. U. *Nano Res.* **2010**, *3*, 738.
- (21) Radha, B.; Kulkarni, G. U. *Cryst. Growth Des.* **2010**, *11*, 320.
- (22) Bhuvana, T.; Smith, K. C.; Fisher, T. S.; Kulkarni, G. U. *Nanoscale* **2009**, *1*, 271.
- (23) Kato, K. J. *Japan Soc. Mech. Eng.* **1915**, *19*, 41.
- (24) Thelander, C.; Dick, K. A.; Borgström, M. T.; Fröberg, L. E.; Caroff, P.; Nilsson, H. A.; Samuelson, L. *Nanotechnology* **2010**, *21*, 205703.
- (25) Rubio-Bollinger, G.; Bahn, S. R.; Agrait, N.; Jacobsen, K. W.; Vieira, S. *Phys. Rev. Lett.* **2001**, *87*, 026101.
- (26) Metzger, R. M. *J. Mater. Chem.* **2008**, *18*, 4364.
- (27) Krumbein, S. J. *IEEE Trans. Compon., Hybrids, Manuf. Technol.* **1988**, *11*, 5.
- (28) Klein, B. J. *J. Phys. F: Met. Phys.* **1973**, *3*, 691.
- (29) Meister, S.; Schoen, D. T.; Topinka, M. A.; Minor, A. M.; Cui, Y. *Nano Lett.* **2008**, *8*, 4562.